Ann. N.Y. Acad. Sci. ISSN 0077-8923

ANNALS OF THE NEW YORK ACADEMY OF SCIENCES

Original Article

Circular RNA circ_0001459 accelerates hepatocellular carcinoma progression via the miR-6165/IGF1R axis

Duo Shen,[1,a] Hongyu Zhao,[2,a] Peng Zeng,[1,a] Meiling Ge,[3] Sachinmulmi Shrestha,[1] and Wei Zhao[1]

[1]Medical School, Southeast University, Nanjing, China. [2]Department of Clinical Research Center, The Second Hospital of Nanjing, Nanjing University of Chinese Medicine, Nanjing, China. [3]Department of Clinical Research Center, Drum Tower Hospital of Nanjing, Nanjing, China

Address for correspondence: Wei Zhao, Medical School, Southeast University, No. 87, Dingjiaqiao Road, Gulou, Nanjing 210000, China. weizhaoseu@163.com

An increasing amount of evidence shows that circular RNAs (circRNAs) have critical effects on cancer progression and development; however, the biological function and potential molecular mechanism of circRNAs in hepatocellular carcinoma (HCC) are still unclear. CircRNA sequencing was used to identify differentially expressed circRNAs between HCC tissue and adjacent normal tissue. We found that circ_0001459 expression was significantly elevated in HCC tissue and cell lines. Furthermore, *in vitro* and *in vivo* functional experiments were carried out to detect the effects of circ_0001459 on HCC growth and metastasis. Knockdown of circ_0001459 significantly inhibited the proliferation, migration, and invasion of HCC cells, whereas upregulation of circ_0001459 had the opposite effect. Moreover, bioinformatics analysis, dual-luciferase reporter assay, RNA immunoprecipitation, and fluorescence *in situ* hybridization assays were used to predict and verify the interaction between circ_0001459, miR-6165, and the target gene IGF1R. Downregulation of circ_0001459 decreased IGF1R expression and inhibited epithelial-to-mesenchymal transition, which could be rescued by treatment with a miR-6165 inhibitor. Mechanistically, we revealed that circ_0001459 could sponge miR-6165 and induce the upregulation of its downstream target IGF1R, thus significantly promoting the progression of HCC. Therefore, circ_0001459 could be a new potential therapeutic target for HCC patients.

Keywords: circ_0001459; HCC; miR-6165; IGF1R; EMT

Introduction

Hepatocellular carcinoma (HCC) is one of the most prevalent cancers and a main cause of cancer-related death worldwide, and its incidence rate and mortality rate are on the rise.[1] Although advancements have been made in mechanistic research and the clinical treatment of HCC, the prognosis of patients with HCC is still poor, and the 5-year survival rate is less than 25%.[2] Hence, it is vital to further investigate the specific molecular mechanism of HCC to identify new effective biomarkers and therapeutic targets.

In recent years, growing evidence has supported the biological function of circular RNAs (circRNAs) in the progression of cancers.[3] CircRNAs are noncoding RNAs with covalent closed loops and are abundant, highly conserved, and relatively stable in the eukaryotic transcriptome.[4,5] It has been reported that circRNAs can participate in the regulation of tumor development and progression through the competitive binding of miRNAs, RNA-binding proteins, and protein-coding RNAs.[6] In addition, a large number of studies have shown that

[a]These authors contributed equally to this work.

doi: 10.1111/nyas.14753

Ann. N.Y. Acad. Sci. 1512 (2022) 46–60 © 2022 The Authors. *Annals of the New York Academy of Sciences* published by Wiley Periodicals LLC on behalf of New York Academy of Sciences.

circRNAs could be used as diagnostic markers and therapeutic targets for cancers.[7–9] For example, circREPS2 regulates the RUNX3/β-catenin pathway by adsorbing miR-558 to inhibit the progression of gastric cancer, and circREPS2 might be a promising biomarker and therapeutic target.[7] CircACTN4 can compete with FUBP1 and block the binding of FUBP1 with FIR, thereby promoting the transcription of MYC and the progression of breast cancer; therefore, circACTN4 might be a new therapeutic target.[8] Circ_0001955 affects the miR-145-5p/NRAS axis in HCC and could act as a promising target for the treatment of HCC.[9] MicroRNAs (miRNAs) are small noncoding RNAs that can directly regulate the levels of most mRNAs.[10] It has been found that the expression of miR-6165 is downregulated in cancers and is related to the progression of cancers.[11,12] However, its effect on HCC remains unclear. Furthermore, insulin-like growth factor 1 receptor (IGF1R) plays a cancer-promoting role in a variety of cancers, including HCC.[13–15]

In this work, we first identified that circ_0001459 was upregulated in HCC tissue and cell lines and had vital effects on promoting HCC progression by binding miR-6165 and upregulating IGF1R expression. Therefore, our findings provide new insight into the mechanism of circ_0001459 in HCC progression and indicate that it might be a promising therapeutic target for HCC.

Materials and methods

Human tissue samples

Thirty-eight pairs of HCC tissue and adjacent normal tissue were obtained during surgical resection. These tissues were stored in liquid nitrogen until further analysis. No patients received any chemotherapy or radiotherapy before the operation and were confirmed to have HCC by pathological diagnosis. This study was approved by the ethics review committee of Nanjing Second Hospital (No. 2020-SL-ky024) and the ethics review committee of Nanjing Drum Tower Hospital (No. 2013-081-05). Patients provided written informed consent before participation.

Cell culture and cell transfection

Human HCC cell lines (HepG2, Huh7, Hep-3B, SK-HEP-1, and SMMC7721) and the immortalized human hepatocyte cell line LO2 were purchased from the Cell Bank of Chinese Academy of Medical Sciences. The cells were cultured in Dulbecco's modified Eagle's medium (DMEM; Gibco, Waltham, MA) supplemented with 10% fetal bovine serum (FBS; Gibco), 100 μg/mL penicillin, and 100 μg/mL streptomycin at 37 °C in 5% CO_2. ShRNA against circ_0001459 (sh-circ), shRNA against negative control (sh-NC), and pcDNA IGF1R overexpression plasmid and its control (pcDNA) were synthesized by GenePharma (China). The pcDNA-based circ_0001459 overexpression vector and pcDNA vector were obtained from GENESEED (China). MiR-6165 mimic, negative control mimic (NC mimic), miR-6165 inhibitor, and negative control inhibitor (NC inhibitor) were obtained from RiboBio (China). Lipofectamine® 3000 (Invitrogen) was used for cell transfection. The sequences of the shRNAs were as follows: sh-circ_0001459#1: TGGATATTCTAACAGATTC; sh-circ_0001459#2: TTCTAACAGATTCAGTGCT; sh-circ_0001459#3: AACAGATTCAGTGCTCAAG; sh-NC: TTCTCCGAACGTGTCACGT.

RNA sequencing

Four pairs of HCC tissue and adjacent normal tissue were randomly selected for RNA sequencing analysis, which was done by Aksomics (China). RNA concentration was determined using a Nano Drop ND-1000. After the total RNA sample was enriched with oligo dT (rRNA removal), the KAPA Stranded RNA-Seq Library Prep Kit (Illumina) was used to construct the library. The dUTP method combined with subsequent high-fidelity PCR polymerase processing was used to synthesize the double-stranded cDNA in the library construction, so that the final RNA sequencing library chain has specificity. An Agilent 2100 Bioanalyzer was used to determine the library quality, and then the library was quantified through qPCR. An Illumina HiSeq 4000 sequencer was used to sequence the mixed library of different samples. Image processing and basic recognition were carried out through Solexa pipeline version 1.8 (Off-Line Base Caller software, version 1.8) software. After removing adapters, the sequencing quality of reads was evaluated by FastQC software. FPKM at gene level and transcription level was calculated by R software Ballgown. New gene/transcript predictions were assembled for each sample through StringTie and compared with the official annotation information, which were

obtained by Ballgown calculation. STAR software was used to compare circRNAs and the reference genome. Detection of backsplice junction reads and read count statistics were performed using CIRCexplorer2. Differential expression calculation was performed by the R software edge R.

RNA extraction, RNase R treatment, and qRT-PCR

Total RNA from HCC tissue and cells was extracted using TRIzol® reagent (Invitrogen). RNase R (3 U/μg) (Epicentre Biotechnologies) was used to digest the total RNA (5 μg) at 37 °C for 15 minutes. qRT-PCR for circRNAs and mRNAs was performed using a StepOne™ Real-Time PCR System and SYBR® Green Mix (TaKaRa, Japan). qRT-PCR for miRNAs was performed using the Mir-X miRNA First-Strand Synthesis Kit (TaKaRa). All primers in this study were synthesized by RiboBio. The expression levels of circRNAs/mRNAs and miRNAs were normalized to the levels of GAPDH and U6, respectively. Primers are shown in Table S1 (online only).

Cell proliferation assays

A total of 2×10^3 cells from different groups were inoculated into each well of a 96-well plate, and cell proliferation was detected by the Cell Counting Kit-8 (CCK-8; Dojindo) assay. After incubation at 37 °C for 2 h, the optical density values were measured at 450 nm. For the colony formation test, a total of 500 HCC cells were inoculated into six-well plates and cultured for 14 days. The cells were fixed with 4% paraformaldehyde for 15 min and stained with 0.1% crystal violet solution for 15 minutes.

EdU assay

For the EdU assay, cells from different groups were cultured with 50 nmol/L EdU (RiboBio) for 2 h and fixed with 4% formaldehyde. Then, 1 mL of Cell LightTM EdU Apollo® 488 (RiboBio) was used to treat the cells. Nuclear staining was performed with DAPI for 30 minutes. The fluorescence intensity was measured with an inverted microscope.

Wound healing assay

Cells from different groups were cultured in six-well plates. In the middle of the well, a scratch was made with a pipette tip, and then the cells were washed with PBS. The average distance between the two sides of the scratch was measured with a caliper to assess the scratch distance at 0 and 48 hours.

Cell migration and invasion assays

Transwell analysis was performed by adding cells to transwell chambers coated with or without Matrigel® (BD Biosciences). After transfection, the cells in each group were counted. A total of 5×10^4 cells from different groups were added to 200 μL of serum-free medium, mixed, and then added to the upper chamber of the transwell chamber. In the invasion test, the upper cavity of the insert was coated with 50 μL Matrigel. After 24 h of culture, the cells were fixed with 4% paraformaldehyde and stained with 0.1% crystal violet for 15 minutes. Finally, five random fields were selected for observation to quantify the number of cells remaining on the lower side.

Flow cytometric analysis of the cell cycle

HepG2 cells and Huh7 cells were cultured in medium without FBS for 12 h and fixed with 70% ethanol at 4 °C for 6 hours. Then, after washing with PBS, the fixed cells were incubated with propidium iodide containing RNase A at room temperature for 30 minutes. Flow cytometry (BD Biosciences) was used to analyze the stained cells.

RNA fluorescence in situ *hybridization*

Cy3-labeled probe sequences for circ_0001459 and FITC-labeled probe sequences for miR-6165 were synthesized by GENESEED and were used to analyze the localization of circ_0001459 and its colocalization with miR-6165 in HepG2 cells and Huh7 cells. Hybridization was performed overnight by using circ_0001459 and miR-6165 probes, and all images were obtained using a laser confocal microscope.

Dual-luciferase reporter gene assay

Fragments of circ_0001459 and IGF1R containing miR-6165 binding sites were purchased from RiboBio and named circ_0001459 wild-type (circ_0001459-WT), IGF1R wild-type (IGF1R-WT), circ_0001459 mutant-type (circ_0001459-MUT), and IGF1R mutant-type (IGF1R-MUT). The WT and MUT fragments were subcloned into the pGL3 promoter vector (GenePharma). HepG2 and Huh7 cells were cultured in 24-well plates and cotransfected with miR-6165 mimic, inhibitor, the relevant negative control, and circ_0001459-WT/circ_0001459-MUT or IGF1R-WT/IGF1R-MUT. Forty-eight hours after transfection, the luciferase activity was measured

by a dual-luciferase reporter assay kit (Promega, Madison, WI).

RNA immunoprecipitation

The RNA immunoprecipitation (RIP) test was performed using the EZ-Magna RIP Kit (Millipore, Billerica, MA) following the manufacturer's protocol. HepG2 and Huh7 cells were collected 48 h after transfection of miR-6165 mimic or the relevant negative control. The cells were lysed in complete RNA lysis buffer and incubated with magnetic beads conjugated with anti-AGO2 antibody (Abcam, Waltham, MA) or negative control IgG antibody (Abcam). The beads were then washed, and the immunoprecipitated RNA was purified and enriched. The purified RNA was measured by qRT-PCR.

RNA pull-down assay

About 1×10^7 cells were collected and lysed in lysis buffer. The lysate was then centrifuged and the supernatant was mixed with the biotin-labeled circ_0001459 probe and the negative control probe (RioBio) at room temperature for 4 hours. Dynabeads^{TM} M-280 Streptavidin (Invitrogen) were used for pull-down assay. The Dynabeads were washed and treated with DNase/RNase-free solutions, and the probes were incubated with the streptavidin-coupled Dynabeads at room temperature for 30 minutes. After the probe-bound Dynabeads were generated, the supernatant was incubated with the coated beads. The mixture was washed and then disrupted with lysis buffer and proteinase K. The RNA complexes bound to the beads were extracted using the RNeasy Mini Kit (Qiagen) for qRT-PCR assay.

Western blotting

Radioimmunoprecipitation assay lysis buffer (Beyotime) was used to extract the proteins from cells and tissues. The proteins were then separated on 10% sodium dodecyl sulfate polyacrylamide gels and transferred to polyvinylidene fluoride membranes (Millipore). The membranes were blocked in 5% nonfat milk for 1 h and incubated with primary antibodies. The primary antibodies included those against IGF1R (1:300, Abcam), Akt (1:1000, Cell Signaling), p-Akt (1:1000, Cell Signaling), P27 (1:1000, Abcam), Bcl-2 (1:800, Abcam), E-cadherin (1:2000, ProteinTech), N-cadherin (1:2000, ProteinTech), vimentin (1:2000, ProteinTech), and GAPDH (1:1000, Abcam), which were incubated at 4 °C overnight. Afterward, the membranes were incubated with secondary antibody for 1 hour. Finally, enhanced chemiluminescence reagent was used to visualize the protein bands.

Immunohistochemistry

The tumor tissues of nude mice were sectioned and fixed with 4% paraformaldehyde for 48 hours. The thickness of the paraffin sections was 5 μm, and the sections were deparaffinized. The sections were blocked with 5% goat serum and then incubated with IGF1R (1:100; Abcam) and Ki-67 (1:200; Abcam) antibodies. Afterward, the sections were cultured at 37 °C for 2 h with the secondary antibody (1:500; Santa Cruz).

Tumor formation in vivo

Five-week-old male BALB/c nude mice were subcutaneously inoculated in the flank with 1×10^7 stably transfected Huh7 cells (sh-circ_0001459 or sh-NC). The tumor volume (V) was checked every 5 days before sacrificing the mice and calculated according to the following formula: $V = \text{length} \times \text{width}^2 \times 0.5$. Approximately 25 days later, the mice were sacrificed, and the tumor tissues were removed and photographed. In addition, the tumor tissues were weighed and stored in liquid nitrogen until further study. A total of 2×10^6 stably transfected Huh7 cells (sh-circ_0001459 or sh-NC) were injected into the tail vein of each mouse, and a model of lung metastasis was established. After 8 weeks, the mice were sacrificed, and then the lungs were stained with hematoxylin and eosin. The mice were maintained, and experiments were carried out in the specific-pathogen-free Animal Laboratory of Southeast University. The animal experimental procedure was approved by the Ethics Committee for Experimental Animals of Southeast University (No. 20210226002).

Statistical analysis

Statistical analysis was performed using SPSS (IBM, version 22.0) or GraphPad Prism® (Version 8.0). Student's *t*-test and one-way ANOVA were used to test the differences between groups. Pearson's correlation coefficient was used in the correlation analysis. All data are expressed as the mean ± standard deviation of at least three independent experiments, and $P < 0.05$ was considered to indicate a statistically significant difference.

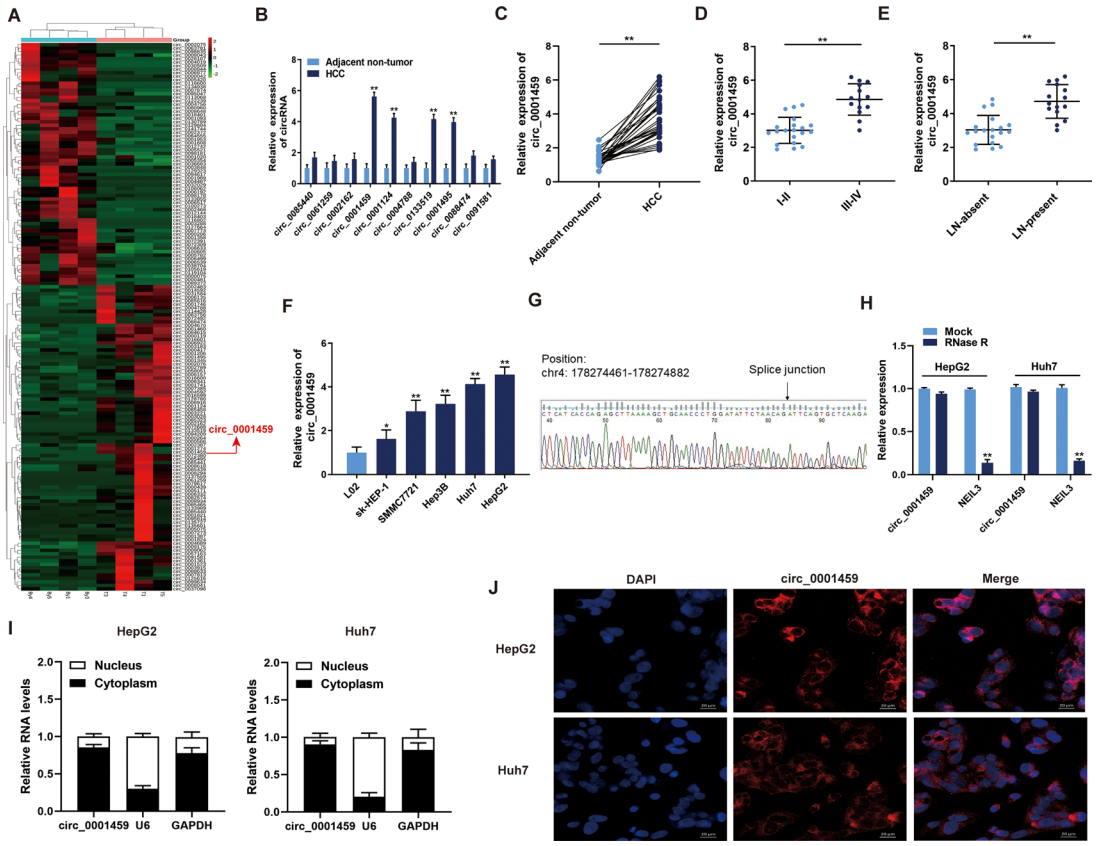

Figure 1. Circ_0001459 is upregulated in HCC. (A) Heatmap of differentially expressed circRNAs in HCC and adjacent normal tissues. (B) Relative expression of circRNAs differentially expressed in 10 pairs of HCC and adjacent normal tissues by qRT-PCR. (C) Relative expression of circ_0001459 in tissues by qRT-PCR. (D) Relative expression of circ_0001459 in HCC tissue at different TNM stages. (E) Relative expression of circ_0001459 in HCC tissue with or without lymph node metastasis. (F) Relative expression of circ_0001459 in cell lines by qRT-PCR. (G) The back-splice junction of circ_0001459 was identified by Sanger sequencing. (H) RNase R digestion was conducted to evaluate the stability of circ_0001459. (I) The expression of circ_0001459 in cytoplasm or nuclear in HCC cells by qRT-PCR. (J) The localization of circ_0001459 was detected by FISH. $^{*}P < 0.05$ and $^{**}P < 0.01$.

Results

Relative circ_0001459 expression levels in HCC

To generate the expression profiles of circRNAs and identify differentially expressed circRNAs in HCC patients, representative paired HCC tissue and adjacent normal tissue from four patients were selected for RNA sequencing. Using the cutoff criteria of fold change >1.5 and P value < 0.05, 183 differentially expressed circRNAs were identified, of which 94 were upregulated and 89 were downregulated (Fig. 1A). qRT-PCR analysis was used to identify the 10 most upregulated circRNAs, and the results indicated that circ_0001459 showed the highest upregulation in another 10 samples of HCC tissue compared with the control tissue (Fig. 1B). Therefore, we selected circ_0001459 for further analysis. To further verify our results, we increased the number of assessed tissue samples to 34 pairs and measured circ_0001459 expression by qRT-PCR. The results showed that the expression level of circ_0001459 in HCC tissue was significantly higher than that in adjacent normal tissue (Fig. 1C). The correlation between circ_0001459 expression level and clinicopathological characteristics in HCC patients is shown in Table S2 (online only). High expression of circ_0001459 was correlated with tumor differentiation and lymph node metastasis. In addition, increased circ_0001459

expression was found in tumor tissues at tumor-node-metastasis (TNM) stages III–IV versus TNM stages I–II (Fig. 1D). Circ_0001459 expression was upregulated in tumor tissues with lymph node metastasis (Fig. 1E). HCC patients with high expression of circ_0001459 displayed shorter overall survival times than those with low expression of circ_0001459, according to Kaplan–Meier survival curve analysis (Fig. S1, online only). Moreover, the expression of circ_0001459 was markedly increased in HCC cell lines (Huh7, HepG2, Hep3B, SMMC7721, and SK-HEP-1) compared with normal LO2 cells (Fig. 1F). The genomic site of circ_0001459 is shown in Figure 1G, and the spliced mature sequence length of circ_0001459 is 131 bp. HepG2 and Huh7 cells were treated with RNase R exonuclease to verify that circ_0001459 was resistant to RNase R, while NEIL3 mRNA was decreased significantly after RNase R treatment (Fig. 1H). Nuclear–cytoplasmic fractionation and RNA fluorescence *in situ* hybridization (FISH) analysis showed that circ_0001459 was mainly located in the cytoplasm (Fig. 1I and J). These results suggested that the expression of circ_0001459 was increased in HCC and may be involved in the progression of HCC.

Circ_0001459 promotes the growth, migration, and invasion of HCC cells

To investigate the biological function of circ_0001459 in HCC cells, three shRNAs (sh-circ_0001459#1, sh-circ_0001459#2, and sh-circ_0001459#3) and an overexpression vector of circ_0001459 were constructed. We measured circ_0001459 expression, and the results revealed that the circ_0001459 expression level was markedly downregulated and upregulated in HepG2 and Huh7 cells, respectively, while the NEIL3 mRNA level did not change (Fig. 2A and B). Among the shRNAs, sh-circ_0001459#1 had the best knockdown efficiency, so it was used for further functional experiments. CCK-8, colony formation, and EdU assays were conducted to assess cell proliferation, and the results indicated that the downregulation of circ_0001459 significantly inhibited cell growth, whereas the upregulation of circ_0001459 promoted cell proliferation (Fig. 2C–E). In the wound healing and transwell assays, the results revealed that circ_0001459 knockdown reduced the migration and invasion of HepG2 and Huh7 cells, while circ_0001459 overexpression showed the opposite effect (Fig. 2F and G). Flow cytometry results revealed that circ_0001459 downregulation induced G1/S phase arrest, whereas circ_0001459 upregulation showed the opposite change (Fig. 2H). Taken together, our results revealed that circ_0001459 exerted a pro-oncogenic effect in HCC cells.

Circ_0001459 functions as a sponge of miR-6165

One of the important biological functions of circRNAs is their role as miRNA sponges. In this study, circ_0001459 was found to be mainly enriched in the cytoplasm, so we speculated that circ_0001459 may play an important biological role in HCC as a miRNA sponge. To verify our hypothesis, the potential target miRNAs were predicted by three bioinformatics databases (TargetScan, miRanda, and RNAhybrid), and a total of five miRNAs were selected from the overlap between the three databases: miR-1301-3p, miR-1914-3p, miR-296-3p, miR-6165, and miR-8069. The expression changes in the five miRNAs in response to circ_0001459 knockdown in HepG2 and Huh7 cells were then measured by qRT-PCR. The results revealed that miR-6165 expression was the most affected by circ_0001459 downregulation (Fig. 3A). Bioinformatic analysis showed that circ_0001459 contains complementary binding sites for miR-6165 (Fig. 3B). Dual-luciferase reporter analysis confirmed that miR-6165 mimics markedly decreased luciferase activity in the wild-type group, while luciferase activity in the mutant group was not affected, suggesting that there may be a direct interaction between miR-6165 and circ_0001459 (Fig. 3C). An anti-AGO2 RIP assay was performed, and the results revealed that circ_0001459 and miR-6165 were pulled down by anti-AGO2 antibody but not IgG (Fig. 3D). An RNA pull-down assay showed a greater enrichment of miR-6165 in the biotinylated-circ_0001459 probe compared with that in the control group (Fig. 3E). Circ_0001459 and miR-6165 were colocalized in the cytoplasm of HepG2 and Huh7 cells according to FISH analysis (Fig. 3F). In contrast with circ_0001459, miR-6165 was significantly downregulated in HCC cell lines and tissues (Fig. 3G and H). The expression of miR-6165 was negatively correlated with the expression of circ_0001459 by

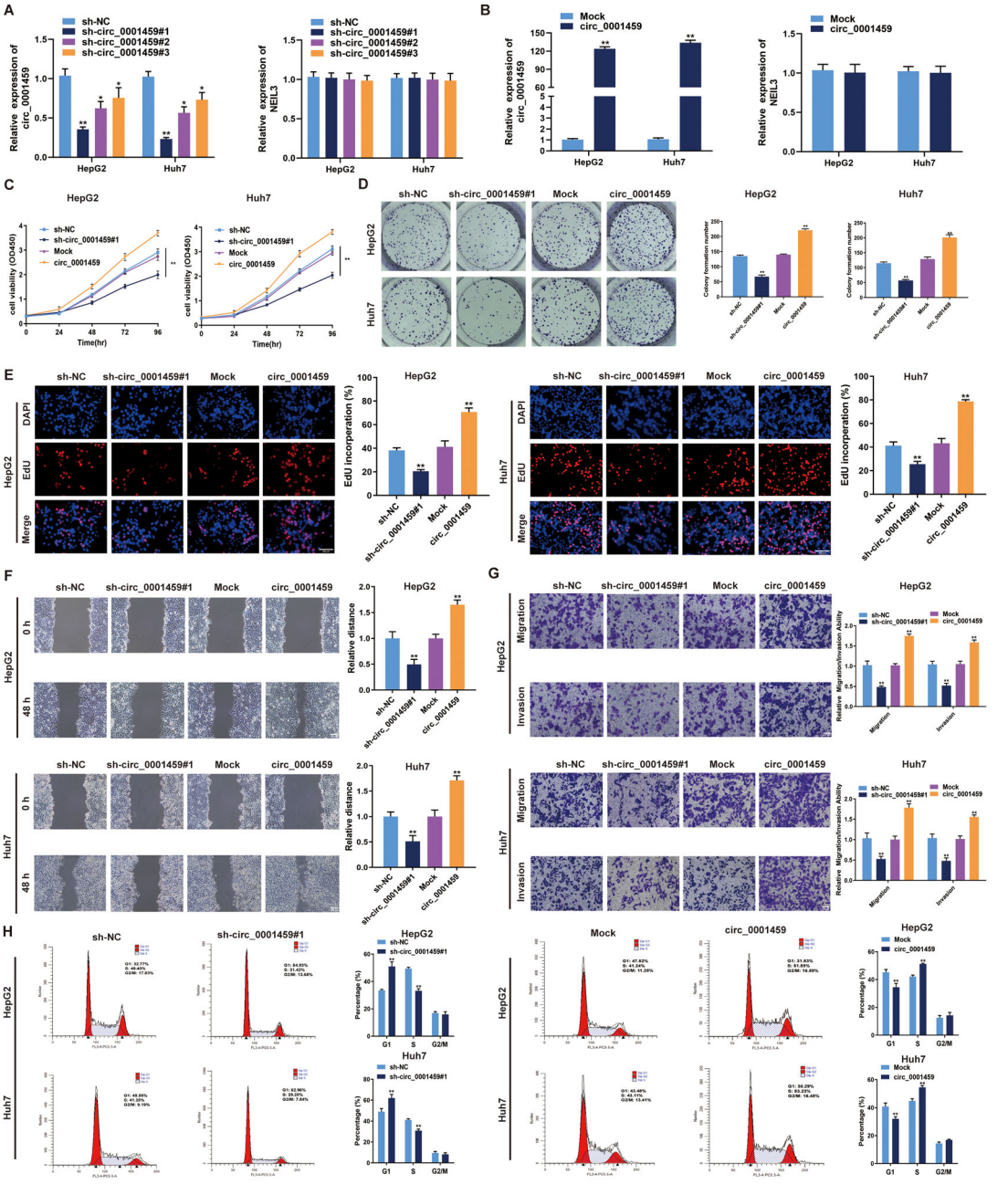

Figure 2. Circ_0001459 promotes the growth, invasion, and migration of HCC cells *in vitro*. (A and B) The effects of knockdown or overexpression of circ_0001459 in HCC cells were measured using qRT-PCR. (C–E) CCK-8, colony formation, and EdU assays of HCC cells with circ_0001459 knockdown or overexpression. (F and G) Wound healing and transwell assays showed that invasion and migration were significantly increased after circ_0001459 overexpression, but inhibited after circ_0001459 knockdown. (H) Flow cytometry analysis was carried out to determine the changes in the cell cycle profile following circ_0001459 knockdown or overexpression in HCC cells. $^{*}P < 0.05$ and $^{**}P < 0.01$.

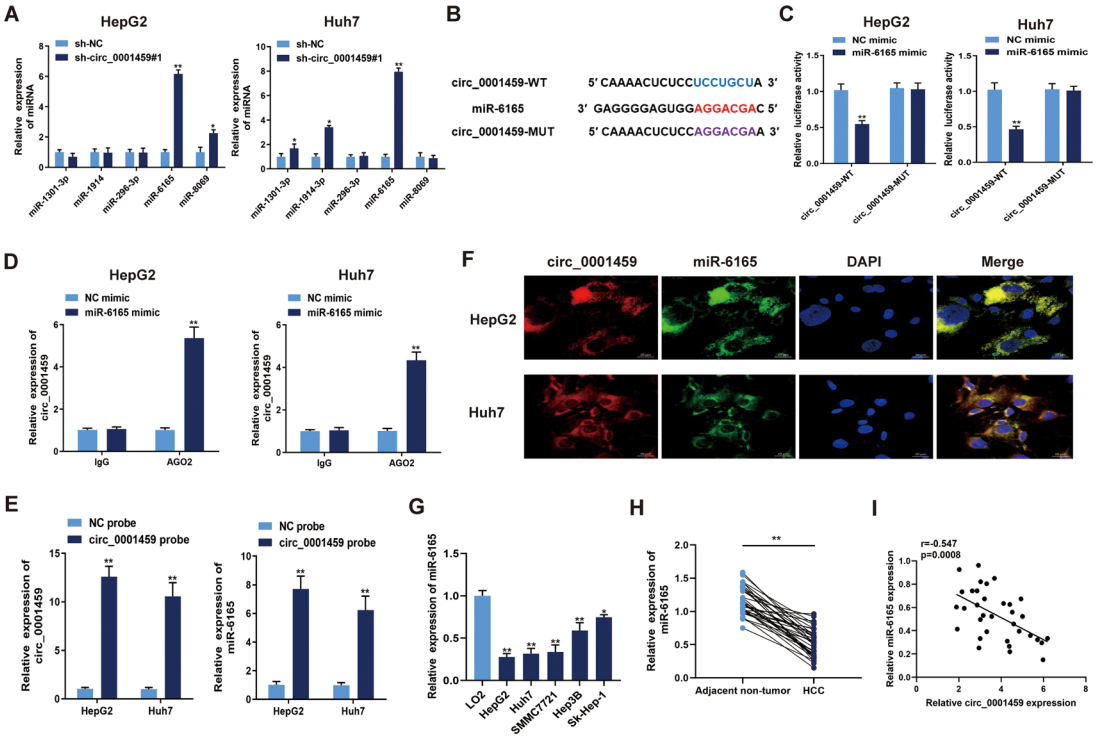

Figure 3. Circ_0001459 functions as a sponge of miR-6165. (A) Relative miRNA expression was measured after the transfection of HCC cells. (B and C) The direct binding between circ_0001459 and miR-6165 was analyzed by dual-luciferase reporter assay. (D) AGO-RIP assay in HepG2 and Huh7 cells. (E) RNA pull-down assay in HepG2 and Huh7 cells. (F) FISH assay showing the colocalization of circ_0001459 and miR-6165 in HCC cells. (G) The expression level of miR-6165 in HCC cells. (H) The expression level of miR-6165 in HCC tissue. (I) Correlation between the expression levels of circ_0001459 and miR-6165 in HCC tissues. $^{*}P < 0.05$ and $^{**}P < 0.01$.

Pearson correlation analysis (Fig. 3I). Overall, these data suggested that circ_0001459 could act as a sponge for miR-6165 in HCC.

MiR-6165 reverses the oncogenic effects of circ_0001459

To verify whether circ_0001459 plays an oncogenic role by sponging miR-6165, rescue experiments using miR-6165 mimics or inhibitors were performed. CCK-8, colony formation, and EdU assays revealed that the miR-6165 inhibitor reversed the inhibitory effect induced by circ_0001459 downregulation in HepG2 cells, whereas miR-6165 mimics counteracted the proliferation-promoting role of circ_0001459 overexpression in Huh7 cells (Fig. 4A–C). Wound healing and transwell experiments showed that downregulation of circ_0001459 inhibited cell migration and invasion, and miR-6165 inhibitor reversed these effects, while overexpression of circ_0001459 significantly enhanced migration and invasion, which could be reversed by miR-6165 mimics (Fig. 4D and E). In conclusion, these findings suggested that miR-6165 may play a vital role downstream of circ_0001459.

IGF1R is a direct target of miR-6165 and is indirectly regulated by circ_0001459

The target genes of miR-6165 were predicted by miRanda, DIANA, TargetScan, and miRmap. Multiple miRNA recognition elements (MREs) for miR-6165 within the 3′-UTR of the IGF1R gene were predicted, and four of the MREs (positions 5871, 6628, 7021, and 8652) revealed the best base pairing score and higher protection state compared with the flanking sequences, underlining their functional importance. A schematic diagram of the base-pairing of the conserved MREs with miR-6165 is shown in Figure 5A. Dual-luciferase reporter analysis was then conducted. The results verified that the luciferase activity of the vector carrying the IGF1R

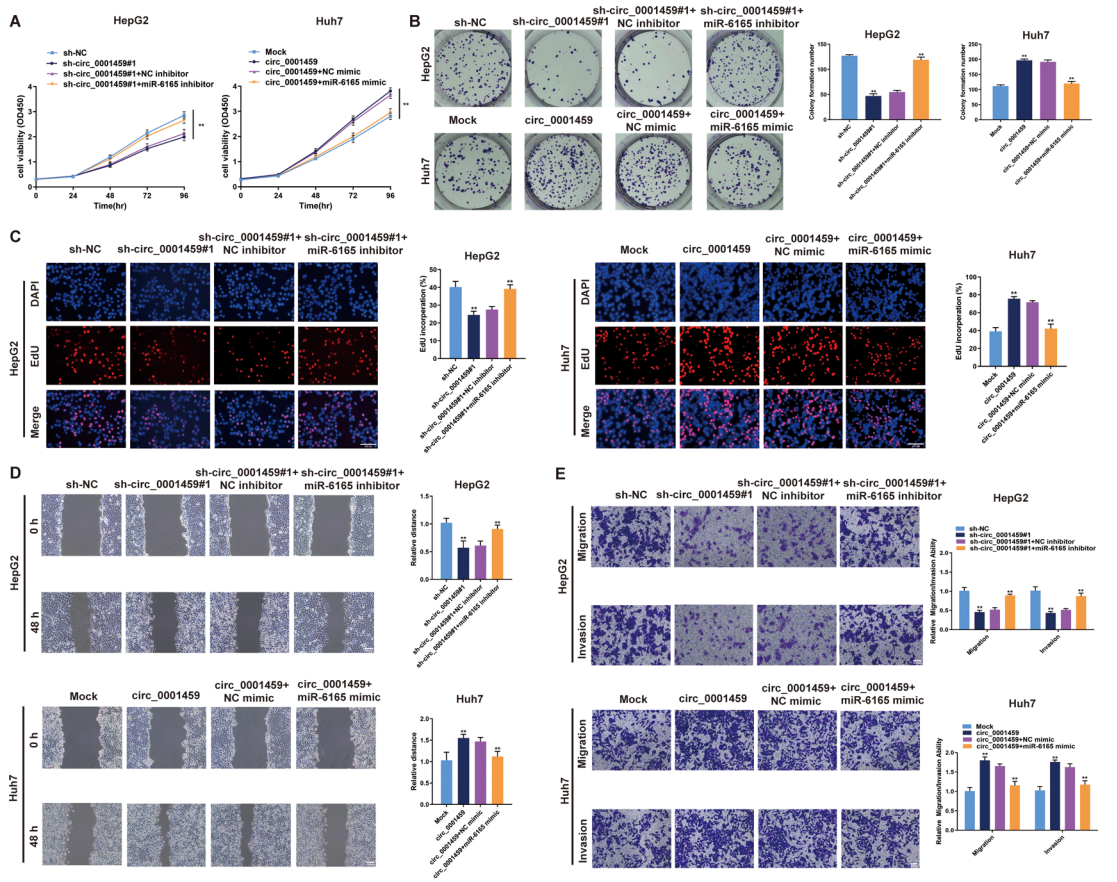

Figure 4. miR-6165 reverses the oncogenic functions of circ_0001459. (A–C) CCK-8, colony formation, and EdU assays revealed that cell proliferation affected by circ_0001459 knockdown or overexpression was reversed by cotransfection with the miR-6165 inhibitor or mimic. (D and E) Wound healing and transwell assays revealed that cell invasion and migration affected by circ_0001459 knockdown or overexpression was reversed by cotransfection with the miR-6165 inhibitor or mimic, respectively. $^{**}P < 0.01$.

wild-type 3′ untranslated region (3′-UTR-WT) was significantly decreased by miR-6165 mimics, while the luciferase activity in the IGF1R mutant 3′-UTR (3′-UTR-MUT) group was not affected (Fig. 5B). The qRT-PCR results showed that the expression of IGF1R was increased significantly in HCC cells and tissues (Fig. 5C). Pearson correlation analysis indicated that the expression of IGF1R was negatively correlated with the expression of miR-6165, as detected by qRT-PCR in 34 paired HCC and normal tissues (Fig. 5D). In addition, qRT-PCR and western blot assays showed that miR-6165 mimics decreased the expression of IGF1R, while miR-6165 inhibitor increased the expression of IGF1R in HCC cells (Fig. 5E and F). Western blot analysis showed that after circ_0001459 knockdown, the expression levels of IGF1R, p-Akt, Bcl-2, N-cadherin, and vimentin were significantly decreased, and the expression levels of p27 and E-cadherin were markedly increased (Fig. 5G). In contrast, overexpression of circ_0001459 had the opposite effect on the expression of these proteins (Fig. 5G). The decrease or increase in IGF1R expression caused by circ_0001459 downregulation or upregulation could be reversed by miR-6165 inhibitor or mimics, respectively (Fig. 5G).

IGF1R overexpression reverses circ_0001459 knockdown-induced inhibition of the growth, migration, and invasion of HCC cells

Since IGF1R is a downstream target of miR-6165 and circ_0001459, we further determined

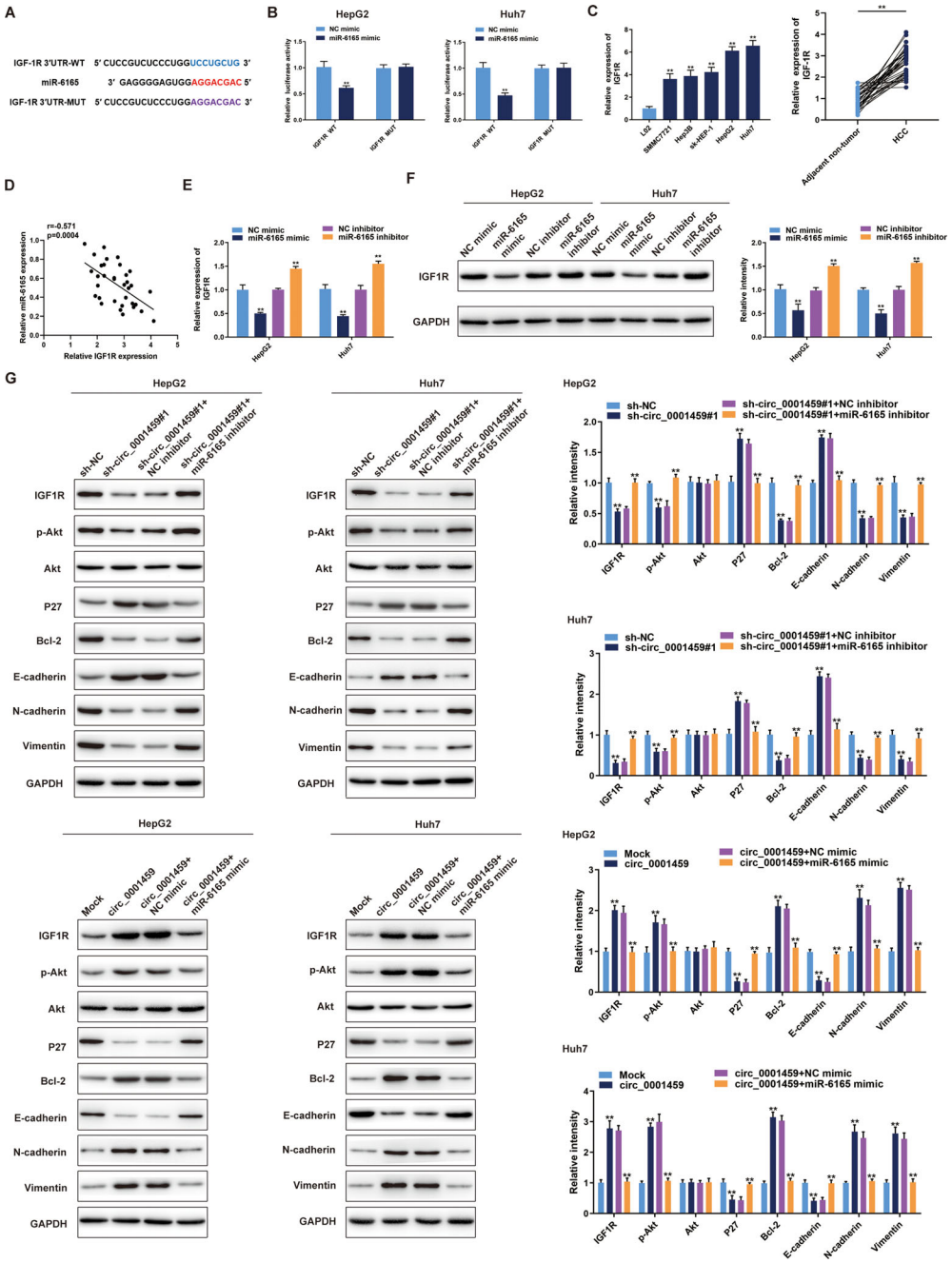

Figure 5. IGF1R is a direct target of miR-6165 and indirectly regulated by circ_0001459. (A) TargetScan showed that miR-6165 could bind to the 3′-UTR of IGF1R. (B) The direct binding between IGF1R 3′-UTR and miR-6165 was analyzed by dual-luciferase reporter assay. (C) The expression level of IGF1R in HCC cells and HCC tissue. (D) Correlation between the expression levels of IGF1R and miR-6165 in HCC tissue. (E and F) The expression level of IGF1R was measured by qRT-PCR and western blotting after transfection of miR-6165 mimic or inhibitor. (G) The protein expression levels of IGF1R and its downstream genes affected by the knockdown or overexpression of circ_0001459 were reversed by cotransfection of the miR-6165 inhibitor or mimic, respectively. $^{**}P < 0.01$.

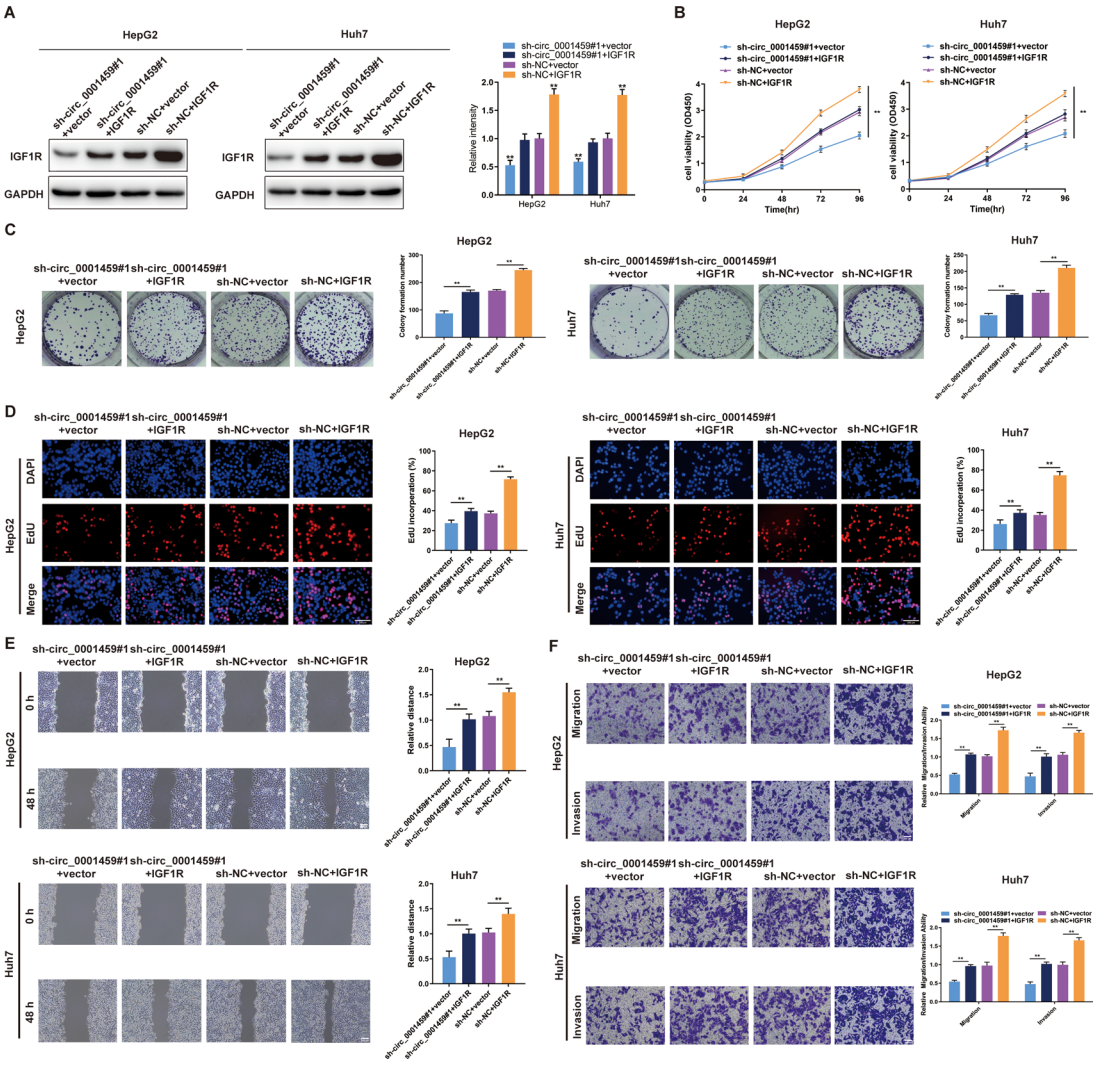

Figure 6. IGF1R overexpression reverses the circ_0001459 knockdown–induced inhibition of proliferation, migration, and invasion of HCC cells. (A) Reduced IGF1R expression induced by circ_0001459 knockdown was markedly reversed by transfecting an IGF1R expression plasmid into HCC cells. (B–D) CCK-8, colony formation, and EdU assays showed that overexpressing IGF1R markedly reversed cell proliferation inhibition induced by silencing circ_0001459. (E and F) Wound healing and transwell assays revealed that overexpressing IGF1R markedly reversed cell invasion and migration inhibition induced by silencing circ_0001459. $^{**}P < 0.01$.

whether circ_0001459 and IGF1R are functionally related. HepG2 and Huh7 cells were cotransfected with sh-circ_0001459#1 (or sh-NC) and the lentiviral vector expressing IGF1R (or control vector). We found that IGF1R overexpression markedly reversed the circ_0001459 knockdown–induced reduction of IGF1R expression in HepG2 and Huh7 cells (Fig. 6A). Using CCK-8, colony formation, EdU, wound healing, and transwell assays, we demonstrated that IGF1R overexpression could promote the proliferation, migration, and invasion of HepG2 and Huh7 cells, and we further observed that IGF1R overexpression could largely block the inhibition of malignant biological behavior after circ_0001459 knockdown (Fig. 6B–F). Altogether, these results suggested that circ_0001459 was involved in HCC progression mainly through targeting IGF1R.

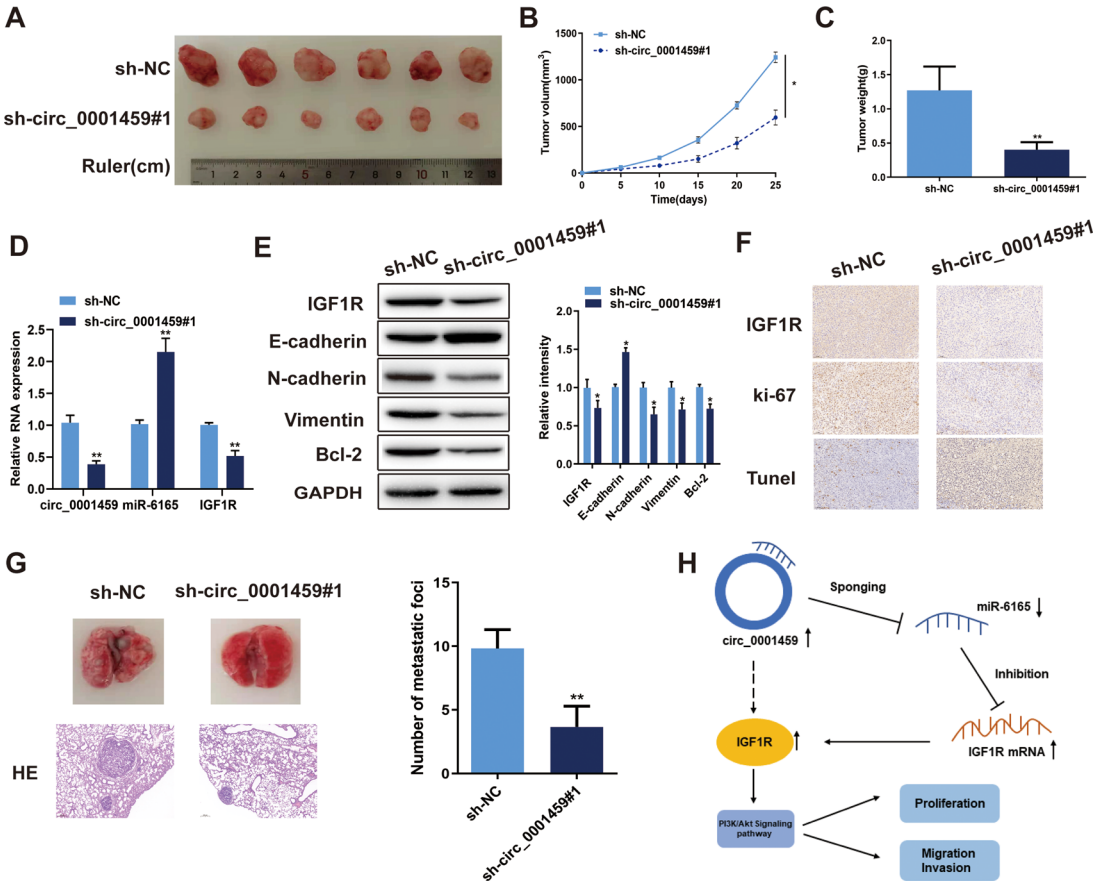

Figure 7. Circ_0001459 promotes tumor growth and lung metastasis *in vivo*. (A) Xenograft tumors in a mouse model of HCC. (B and C) Tumor volumes and tumor weights of the sh-circ_0001459 and sh-NC treatment groups. (D) circ_0001459, miR-6165, and IGF1R levels were detected in the tumor tissue in each group by qRT-PCR. (E) The protein expression levels of IGF1R and its downstream genes were detected in the tumor tissue in each group by western blotting. (F) The expression of IGF1R and Ki-67 in different groups was detected by IHC, and TUNEL staining was performed to detect the apoptotic cells in different groups. (G) The pulmonary nodules from different groups of mice were analyzed by HE staining. (H) Schematic diagram of the mechanism and function of circ_0001459 in HCC progression. $^{*}P < 0.05$ and $^{**}P < 0.01$.

Circ_0001459 promotes tumor growth and lung metastasis in vivo

To reveal the role of circ_0001459 *in vivo*, circ_0001459-knockdown Huh7 cells and negative control cells were injected into the flanks of BALB/c nude mice. The results indicated that circ_0001459 downregulation reduced the tumor size and weight of mice (Fig. 7A–C). In addition, circ_0001459 and IGF1R expression levels were decreased, whereas the miR-6165 level was increased in tumor tissues from the sh-circ_0001459 group compared with the sh-NC group (Fig. 7D). Western blot analysis showed that IGF1R, N-cadherin, vimentin, and Bcl-2 expression levels were decreased, while the E-cadherin expression level was increased in the sh-circ_0001459 group compared with the sh-NC group (Fig. 7E). The IGF1R and Ki-67 expression levels in tumor tissue collected from the sh-circ_0001459 group were decreased compared with those in the sh-NC group, and the sh-circ_0001459 group showed more apoptotic cells (Fig. 7F). After 8 weeks, the mice were euthanized, and their lung tissue was collected for study. The mouse lungs of the sh-circ_0001459 group had fewer metastatic foci than those of the sh-NC group (Fig. 7G). In conclusion, our results

revealed that the circ_0001459/miR-6165/IGF1R pathway promotes the progression of HCC (Fig. 7H).

Discussion

It is generally believed that circRNAs have crucial effects on regulating genes in human cancers.[16] Therefore, understanding the biological roles of circRNAs has become of great interest. For example, circ_0000337 promotes the cisplatin resistance of esophageal cancer via the miR-377-3p/JAK2 pathway, which might be a potential therapeutic target of esophageal cancer.[17] Circ_100146 acts as a tumor promoter in prostate cancer via the miR-615-5p/TRIP13 axis.[18] Circ_0089823 regulates SOX4 by sponging miR-507, miR-557, miR-579-3p, and miR-1287-5p, thereby enhancing the progression of non-small-cell lung cancer.[19] Additionally, circRNAs are associated with HCC. For instance, circRASGRF2 accelerates HCC progression by sponging miR-1224 to upregulate FAK expression.[20] Circ_0014717 may be a promising biomarker for HCC through the miR-668-3p/BTG2 pathway.[21] CircFAM13B promotes the progression of HCC via the miR-212/E2F5 axis and activates the P53 axis.[22] Has_circ_0016788 regulates the proliferation and glycolysis of HCC by sponging miR-506-3p and upregulating PARP14.[23]

In this study, we found that circ_0001459 was significantly enhanced in HCC tissue and cells compared with normal control tissue. To reveal the role of circ_0001459 in HCC, HepG2 cells and Huh7 cells with loss of circ_0001459 expression (mediated by sh-circ_0001459 transfection) were designed, and the effects on the malignant biological function of the cells were examined. The cells with downregulated circ_0001459 expression showed obvious deceases in proliferation, migration, and invasion. Huh7 cells transfected with sh-circ_0001459 were injected subcutaneously into nude mice via the caudal vein. The results revealed that the tumors were significantly smaller in terms of volume and weight and that the number of pulmonary nodules was reduced in the knockdown group versus the control group. These data suggested that circ_0001459 plays an important regulatory role in HCC. Many studies have reported that circRNAs can be used as competing endogenous RNAs (ceRNAs) in the occurrence and progression of human cancers. The role of circRNAs in regulating miRNAs has been an active area of research in recent years. miR-6165 is predicted to be a target of circ_0001459. miR-6165 can inhibit the migration and invasion of gastric cancer by regulating STRN4.[11] miR-6165 is a tumor suppressor in colorectal cancer that can regulate IGF1R expression.[12] The close interaction between miR-6165 and circ_0001459 was confirmed in HCC cells; miR-6165 inhibitor was found to reverse the functional changes in HCC cells caused by circ_0001459 knockdown.

IGF1R is an important signaling molecule involved in many tumor processes.[24–26] For example, long noncoding RNA SNHG11 facilitates prostate cancer progression by upregulating IGF1R expression.[27] IGF1R increases the proliferation and glycolysis of pancreatic cancer.[28] HOXB13 accelerates gastric cancer cell migration and invasion by upregulating the expression of IGF1R.[29] IGF1R is activated through miR-122 downregulation, resulting in activation of the RAS/RAF/ERK pathway in HCC.[30] Based on these data, we examined the expression of IGF1R in HCC tissues and cells. There was a positive correlation between IGF1R and circ_0001459. In HepG2 and Huh7 cells, the deletion of circ_0001459 greatly inhibited the expression of IGF1R. miR-6165 can interact directly with IGF1R by binding to the 3′-UTR of IGF1R. Previous studies have shown that circRNAs, as miRNA sponges, regulate the expression of tumor regulatory genes through the circRNA–miRNA–mRNA axis.[17–19] In our study, we found that circ_0001459 sponged miR-6165 to regulate the expression of IGF1R in HCC. Some circRNAs can accumulate in the nucleus and bind to linear transcripts of parental genes to regulate mRNA translation.[31] Furthermore, some circRNAs can be translated into proteins to play key biological functions.[32] Attention should be focused on the detailed functional mechanism of circ_0001459 in HCC in future studies. Moreover, these studies should include more HCC clinical samples and HCC cell lines. Other specific circRNAs and their detailed mechanisms in HCC also need to be further studied. In conclusion, we found that circ_0001459 was upregulated in HCC and sponged miR-6165 to increase IGF1R expression. The deletion of circ_0001459 could markedly inhibit the progression of HCC cells by targeting the miR-6165/IGF1R axis. Our results identified a new therapeutic target for HCC.

Acknowledgments

This study was supported by the Obstetrics and Gynecology Disease Biobank, Jiangsu Biobank of Clinical Resources (No. BM2015004).

Author contributions

D.S., H.Z., P.Z., and W.Z. designed the experiments. M.G. and S.S. collated the data, carried out data analyses, and produced the initial draft of the manuscript. D.S., H.Z., and P.Z. contributed to drafting of the manuscript. All authors have read and approved the final submitted manuscript.

Supporting information

Additional supporting information may be found in the online version of this article.

Figure S1. Kaplan–Meier analysis showed the level of circ_0001459 was predictive of overall survival in HCC.

Table S1. Primers used for real-time PCR

Table S2. Correlation between circ_0001459 and clinicopathological parameters

Competing interests

The authors declare no competing interests.

Peer review

The peer review history for this article is available at: https://publons.com/publon/10.1111/nyas.14753

References

1. Sayiner, M., P. Golabi & Z.M. Younossi. 2019. Disease burden of hepatocellular carcinoma: a global perspective. *Dig. Dis. Sci.* **64:** 910–917.
2. Bertuccio, P., F. Turati, G. Carioli, *et al.* 2017. Global trends and predictions in hepatocellular carcinoma mortality. *J. Hepatol.* **67:** 302–309.
3. Han, B., J. Chao & H. Yao. 2018. Circular RNA and its mechanisms in disease: from the bench to the clinic. *Pharmacol. Ther.* **187:** 31–44.
4. Kristensen, L.S., M.S. Andersen, L.V.W. Stagsted, *et al.* 2019. The biogenesis, biology and characterization of circular RNAs. *Nat. Rev. Genet.* **20:** 675–691.
5. Patop, I.L., S. Wüst & S. Kadener. 2019. Past, present, and future of circ RNAs. *EMBO J.* **38:** e100836.
6. Shang, Q., Z. Yang & R. Jia. 2019. The novel roles of circRNAs in human cancer. *Mol. Cancer* **18:** 1–10.
7. Guo, X., X. Dai, J. Liu, *et al.* 2020. Circular RNA circREPS2 acts as a sponge of miR-558 to suppress gastric cancer progression by regulating RUNX3/β-catenin signaling. *Mol. Ther. Nucleic Acids* **21:** 577–591.
8. Wang, X., L. Xing, R. Yang, *et al.* 2021. The circACTN4 interacts with FUBP1 to promote tumorigenesis and progression of breast cancer by regulating the expression of proto-oncogene MYC. *Mol. Cancer* **20:** 1–21.
9. Ding, B., W. Fan & W. Lou. 2020. Hsa_circ_0001955 enhances *in vitro* proliferation, migration, and invasion of HCC cells through miR-145-5p/NRAS axis. *Mol. Ther. Nucleic Acids* **22:** 445–455.
10. Mohr, A.M. & J.L. Mott. 2015. Overview of microRNA biology. *Semin. Liver Dis.* **35:** 3–11.
11. Wang, Z., Y. Li, J. Cao, *et al.* 2020. MicroRNA profile identifies miR-6165 could suppress gastric cancer migration and invasion by targeting STRN4. *Onco. Targets Ther.* **13:** 1859–1869.
12. Hassanlou, M., B.M. Soltani, A. Medlej, *et al.* 2020. Hsa-miR-6165 downregulates insulin-like growth factor-1 receptor (IGF-1R) expression and enhances apoptosis in SW480 cells. *Biol. Chem.* **401:** 477–485.
13. Qiao, C., W. Huang, J. Chen, *et al.* 2021. IGF1-mediated HOXA13 overexpression promotes colorectal cancer metastasis through upregulating ACLY and IGF1R. *Cell Death Dis.* **12:** 564.
14. Xu, H., Y. Zhao, X. Gao, *et al.* 2021. An innovative fluorescent probe targeting IGF1R for breast cancer diagnosis. *Eur. J. Med. Chem.* **219:** 113440.
15. Lin, Z., S. Xia, Y. Liang, *et al.* 2020. LXR activation potentiates sorafenib sensitivity in HCC by activating microRNA-378a transcription. *Theranostics* **10:** 8834–8850.
16. Ma, S., S. Kong, F. Wang & S. Ju. 2020. CircRNAs: biogenesis, functions, and role in drug-resistant tumours. *Mol. Cancer* **19:** 1–19.
17. Zang, R., X. Qiu, Y. Song & Y. Wang. 2021. Exosomes mediated transfer of circ_0000337 contributes to cisplatin (CDDP) resistance of esophageal cancer by regulating JAK2 via miR-377-3p. *Front. Cell Dev. Biol.* **9:** 1–13.
18. Zeng, L., Y. Liu, N. Yang, *et al.* 2021. Hsa_circRNA_100146 promotes prostate cancer progression by upregulating TRIP13 via sponging miR-615-5p. *Front. Mol. Biosci.* **8:** 1–9.
19. Li, J., Z. Zhu, S. Li, *et al.* 2021. Circ_0089823 reinforces malignant behaviors of non-small cell lung cancer by acting as a sponge for microRNAs targeting SOX4. *Neoplasia* **23:** 887–897.
20. Wu, D., A. Xia, T. Fan & G. Li. 2021. circRASGRF2 functions as an oncogenic gene in hepatocellular carcinoma by acting as a miR-1224 sponge. *Mol. Ther. Nucleic Acids* **23:** 13–26.
21. Ma, H., C. Huang, Q. Huang, *et al.* 2021. Circular RNA circ_0014717 suppresses hepatocellular carcinoma tumorigenesis through regulating miR-668-3p/BTG2 axis. *Front. Oncol.* **10:** 1–11.
22. Xie, Y., X. Hang, W. Xu, *et al.* 2021. CircFAM13B promotes the proliferation of hepatocellular carcinoma by sponging miR-212, upregulating E2F5 expression and activating the P53 pathway. *Cancer Cell Int.* **21:** 410.
23. Chen, M., G. Hu, X. Zhou, *et al.* 2021. Hsa_circ_0016788 regulates glycolysis and proliferation via miR-506-3p/

PARP14 axis of hepatocellular carcinoma. *J. Gastroenterol. Hepatol.* **36:** 3457–3468.
24. Pollak, M. 2008. Insulin and insulin-like growth factor signalling in neoplasia. *Nat. Rev. Cancer* **8:** 915–928.
25. Tao, Y., V. Pinzi, J. Bourhis & E. Deutsch. 2007. Mechanisms of disease: signaling of the insulin-like growth factor 1 receptor pathway—therapeutic perspectives in cancer. *Nat. Clin. Pract. Oncol.* **4:** 591–602.
26. Casa, A.J., R.K. Dearth, B.C. Litzenburger, *et al.* 2008. The type I insulin-like growth factor receptor pathway: a key player in cancer therapeutic resistance. *Front. Biosci*. **13:** 3273–3287.
27. Xie, Q., S. Zhao, R. Kang & X. Wang. 2021. lncRNA SNHG11 facilitates prostate cancer progression through the upregulation of IGF-1R expression and by sponging miR-184. *Int. J. Mol. Med.* **48:** 182.
28. Hu, L., X. Xu, Q. Li, *et al*. 2021. Caveolin-1 increases glycolysis in pancreatic cancer cells and triggers cachectic states. *FASEB J*. **35:** e21826.
29. Guo, C., H. Chu, Z. Gong, *et al*. 2021. HOXB13 promotes gastric cancer cell migration and invasion via IGF-1R upregulation and subsequent activation of PI3K/AKT/mTOR signaling pathway. *Life Sci*. **278:** 119522.
30. Xu, Y., J. Huang, L. Ma, *et al*. 2016. MicroRNA-122 confers sorafenib resistance to hepatocellular carcinoma cells by targeting IGF-1R to regulate RAS/RAF/ERK signaling pathways. *Cancer Lett*. **371:** 171–181.
31. Pamudurti, N.R., O. Bartok, M. Jens, *et al*. 2017. Translation of circRNAs. *Mol. Cell* **66:** 9–21.
32. Du, W.W., C. Zhang, W. Yang, *et al*. 2017. Identifying and characterizing circRNA–protein interaction. *Theranostics* **7:** 4183–4191.